Reprinted from

MATERIALS SCIENCE AND TECHNOLOGY

The Institute of Materials

Textures of strip cast and hot rolled ferritic and austenitic stainless steel

D. Raabe

Recent progress in strip casting technology allows the production of ferritic and austenitic stainless steels with the same geometry and quality as those provided by conventional hot rolling. This enables the entire hot rolling procedure to be bypassed. The random initial crystallographic orientation distribution through the thickness of the cast strip leads to more homogeneous properties of the final steel sheet. The latter effect eliminates the well known ridging phenomenon in ferritic stainless steel which often deteriorates the surface quality of initially hot rolled bands. In the present paper the crystallographic texture of strip cast ferritic and austenitic stainless steel is examined in various through thickness depths. The results are compared with those for conventionally produced, i.e. continuously cast and subsequently hot rolled specimens. *MST/3010*

 Manuscript received 24 February 1994; in final form 16 May 1994. *The author is in the Institut für Metallkunde und Metallphysik, RWTH Aachen, Germany.*

Introduction

Flat products of highly alloyed ferritic and austenitic stainless steels are conventionally manufactured by continuous casting, hot rolling, hot band annealing, and subsequent pickling, cold rolling, and final recrystallisation. However, recent progress in strip casting technology, in which liquid steel solidifies on the surfaces of two rotating water cooled rolls, provides three main improvements compared with the customary processing method.[1,2] First, it allows the casting of steel sheet with the same thickness and width as that produced by hot rolling. This means that the entire hot rolling process is bypassed. Second, the strip cast material reveals a weak initial crystallographic texture as well as a weak through thickness texture gradient. These features are beneficial for the strength and deep drawing properties of the final sheet. As has been discussed previously,[3,4] the latter is of special relevance for the avoidance of the ridging phenomenon in ferritic stainless steels with 17%Cr content, which considerably affects the surface quality of conventionally produced sheets. Third, it is economically unfavourable to produce small amounts of highly alloyed stainless steel by continuous casting and hot rolling. Strip casting technology is therefore considered to play a competitive role in the future production of stainless steel sheet.

Whereas the texture and microstructure of cold rolled and recrystallised ferritic[5,6] and austenitic[7–9] stainless steels have already been subject to detailed investigations in the past, the microstructural and crystallographic features resulting from hot rolling,[10,11] and especially from strip casting, have not yet been thoroughly discussed in the literature. In the present work, therefore, the crystallographic texture and microstructure of strip cast ferritic and austenitic stainless steel are compared with those of continuously cast and hot rolled material. For this purpose the corresponding measurements are carried out with high spatial resolution at various depths on samples from both alloys.

Experimental

The chemical composition of both steels is given in Table 1. The samples were prepared from conventionally processed hot band as well as from as strip cast material. The latter specimens were industrially produced by casting liquid steel into a preheated tundish, which contacts two rotating water cooled steel rolls. The two casting rolls with different diameters are located as shown in Fig. 1, and the steel solidifies as a thin film on the roll surfaces. The process is controlled in such a manner that the contact length between the liquid metal and the roll surface is equal for both rolls. In the rolling gap the solid films impinge and are compressed to a strip which leaves the gap with a temperature of about 1370 K. A thorough survey of the casting technique is given in Refs. 1–3. The thickness of the ferritic strip cast sample was 4 mm and that of the austenitic sample was 2·4 mm.

Unidirectional hot rolling of continuously cast slab was carried out after reheating and initial reversing hot rolling in a conventional hot strip mill, where the band is deformed in seven subsequent rolling passes. The temperature was in the range 1420–1470 K during the first hot rolling pass, and in the range 1050–1200 K during the last pass. The thickness of the ferritic hot band was 4 mm and that of the austenitic band was 2·2 mm.

Both types of sample (i.e. the conventionally hot rolled as well as the strip cast sheet) were heat treated at 1370 K for 20 min and subsequently descaled before cold rolling.

The crystallographic textures were investigated quantitatively by measuring the four incomplete pole figures {110}, {200}, {112}, and {103} in the ferritic steel and {111}, {200}, {220}, and {113} in the austenitic samples using Mo $K_{\alpha 1}$ radiation in the back reflection mode.[12] From the pole figures the orientation distribution function (ODF) was computed making use of the series expansion method ($l_{max} = 22$).[13] Owing to the cubic crystal symmetry of the steels and the orthorhombic symmetry of the samples (characterised by the rolling (or casting), normal, and transverse directions (RD, ND, TD) respectively), an orientation is represented by the three Euler angles φ_1, ϕ, and φ_2 in the reduced Euler space. For simplicity an orientation is often described using the Miller notation $\{hkl\}\langle uvw\rangle$. In this nomenclature the first indices $\{hkl\}$ describe the crystallographic plane which is parallel to the sheet surface and $\langle uvw\rangle$ indicates the direction that is parallel to RD.

Stainless steels often develop characteristic crystallographic fibre textures during rolling deformation.[3–11] In

Table 1 Chemical compositions of steels investigated (bal. Fe), wt-%

Type of steel	C	Cr	Ni	N	Ti	Nb
Austenitic	0·07	18·0	8·5	0·03	...	...
Ferritic	0·05	16·5	...	0·03	0·01	0·01

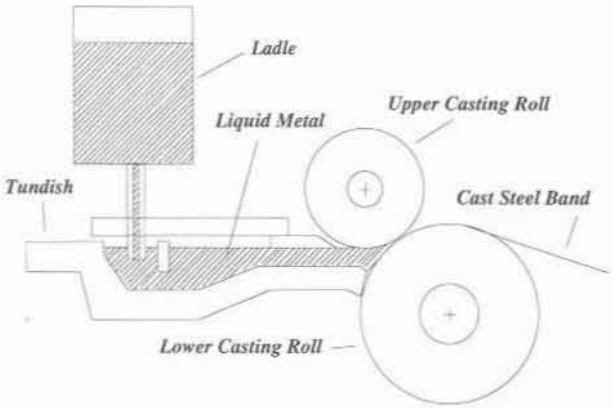

1 Schematic cross-section of strip casting process

many instances it is thus convenient to present the orientation distribution by isointensity diagrams in sections through the Euler space or by fibre diagrams (*see* Table 2). In the first instance the orientation space is subdivided parallel to one Euler axis (for ferritic steels usually φ_1 and for austenitic steels usually φ_2) in 5° steps. In the second instance the orientation density f(g) is given on the ordinate versus one of the angles φ_1, ϕ, or φ_2 while the other two coordinates remain constant. In Fig. 2 the positions of some relevant orientations and texture fibres are schematically presented in φ_1 and φ_2 sections through Euler space.

Since the texture and microstructure, particularly of hot worked stainless steels, is often very inhomogeneous through the thickness,[7] all samples were examined at different depths. To indicate the inspected layer the parameter $s = a/(\frac{1}{2} \times d)$ is defined, where a is the distance from the centre layer and d the thickness of the sheet, i.e. the surface layer is defined by $s = 1$ and the centre layer by $s = 0$. The textures of all samples are examined in $\Delta s = 0{\cdot}1$ through thickness steps. To remove a surface layer of 20 μm (i.e. to remove disturbing grinding effects before the texture measurements), the austenitic samples were etched in a solution of 100 mL H_2O, 100 mL HCl, and 30 mL HNO_3 at a temperature of 330 K. The ferritic samples were etched at room temperature in a solution of 100 mL H_2O_2, 10 mL HF, 5 mL HNO_3, and 5 mL HCl.

Experimental results

MICROSTRUCTURE

The micrographs of the strip cast austenitic steel (transverse section), (Fig. 3) show that compared with the hot rolled material, a more inhomogeneous microstructure through the thickness of the sheet is found. Whereas between the surface and the near centre layers (i.e. between $s = 1$ and $s \approx 0{\cdot}4$) large uniformly oriented blocks of austenitic dendrites can be seen, closer to the centre layers a different microstructure appears. Between $s \approx 0{\cdot}3$ and $s \approx 0{\cdot}1$ a more blocky and nearly equiaxed austenite morphology, which contains martensite plates, has developed. Between $s \approx 0{\cdot}1$ and $s = 0$, i.e. in the midthickness layer of the material, an equiaxed austenitic grain structure with a martensitic volume fraction of up to 20% becomes visible. The same changes in morphology also occur in the strip cast ferritic steel. The differences between the strip cast samples and the hot rolled band can be seen in Fig. 4. Whereas in the subsurface layer of the strip cast austenitic band (Fig. 4*a*) a dendritic zone, which in this micrograph is cut perpendicular to the dendrite axis, can be seen, at the same depth the corresponding austenitic hot band reveals an equiaxed, twinned microstructure (Fig. 4*b*).

Table 2 Relevant orientation fibres for description of textures in stainless steels

Name of fibre	Fibre axis	Orientations on fibre
α fibre (ferrite)	⟨110⟩ ∥ RD	{001}⟨110⟩, {112}⟨110⟩, {111}⟨110⟩
α fibre (austenite)	⟨110⟩ ∥ ND	{110}⟨001⟩, {110}⟨112⟩, {110}⟨111⟩
γ fibre	⟨111⟩ ∥ ND	{111}⟨110⟩,{111}⟨112⟩
β fibre	less symmetric	{112}⟨111⟩, {123}⟨634⟩, {011}⟨211⟩

RD rolling direction; ND normal direction.

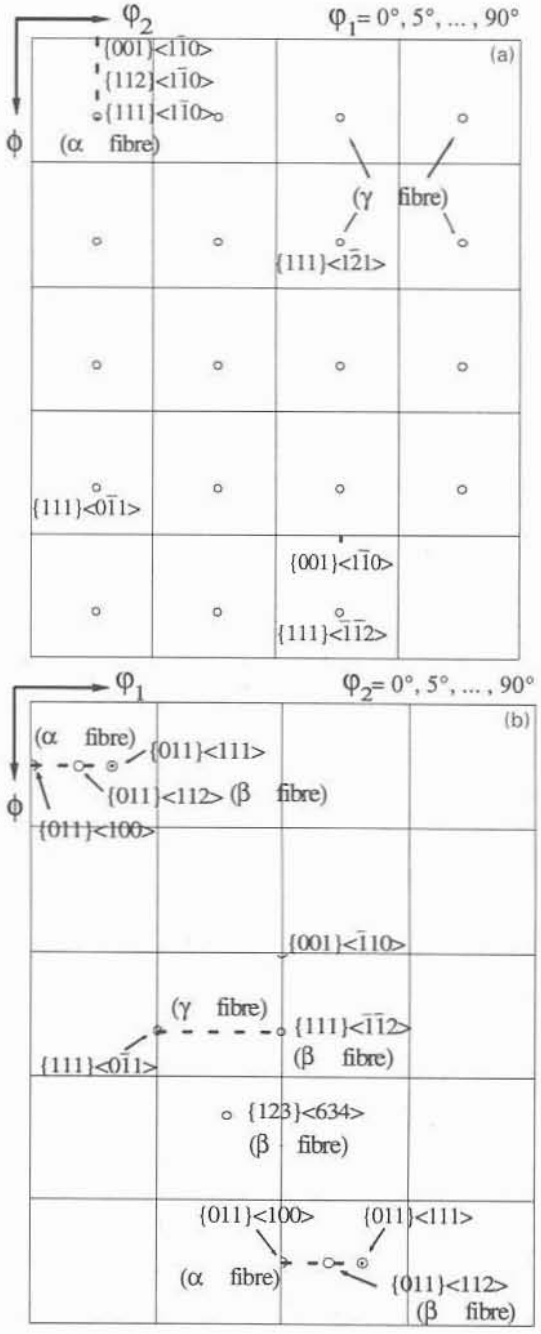

a φ_1 sections, ferritic steel; *b* φ_2 sections, austenitic steel

2 Relevant fibres and orientations in reduced Euler space

TEXTURE

Both types of stainless strip cast material reveal a nearly random orientation distribution in all through thickness layers (*see* Fig. 5). The observed texture gradients are negligible in both alloys when compared with the corresponding hot rolled material. As noted previously,[14] the

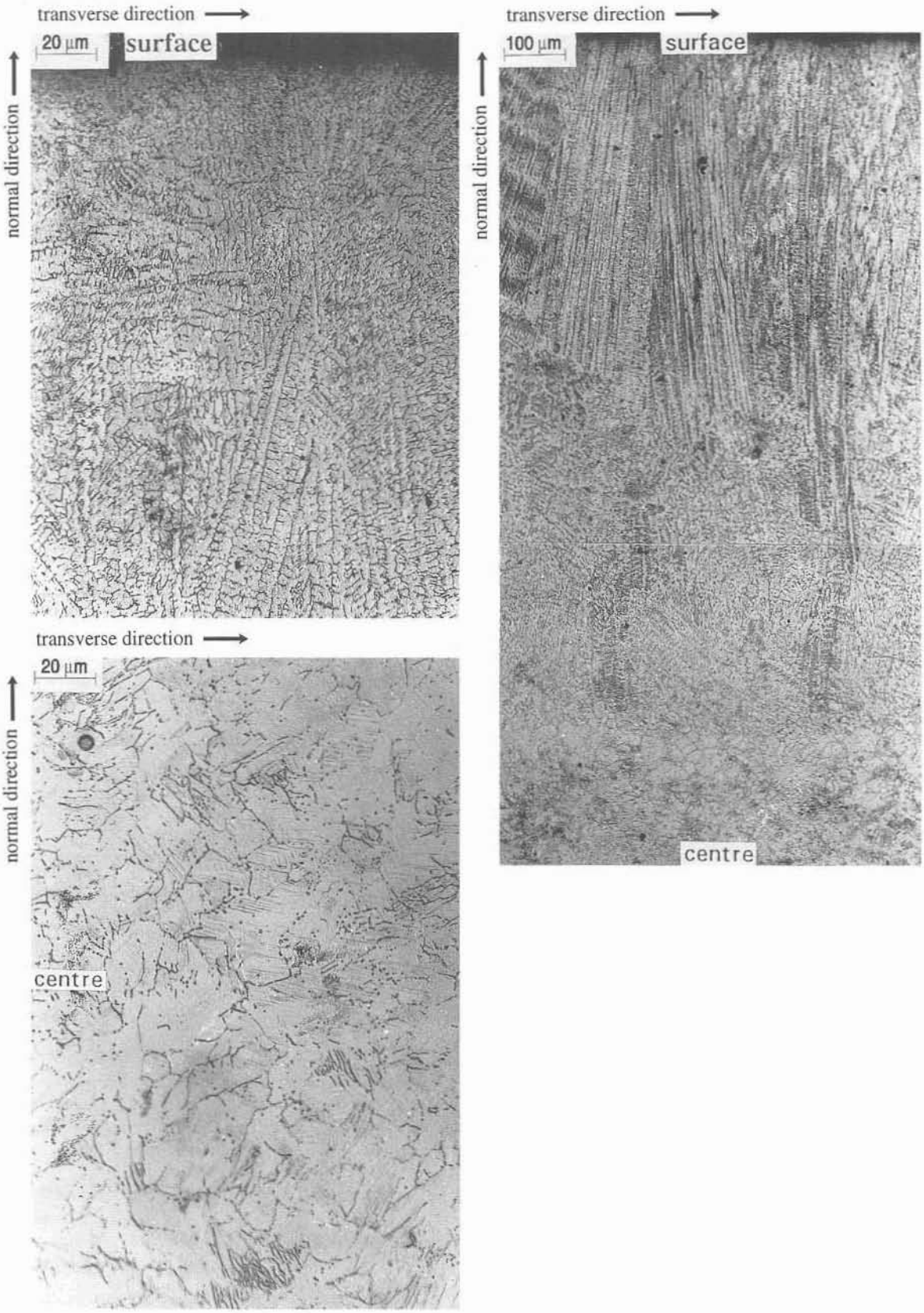

3 Micrographs of austenitic strip cast steel (transverse sections)

strip cast texture is unequal on both sides of the sheet, i.e. the through thickness texture is not symmetric with respect to the centre layer. The nearly random strip casting textures which are found in both alloys are completely different from the textures which result from continuous casting and subsequent hot rolling.

In the centre layer of the hot rolled ferritic steel band, a strong rolling texture consisting of a sharp α fibre and a weaker γ fibre is detected (*see* Fig. 6*a*). At the subsurface layer, a strong shear texture with a maximum at the Goss component, $\{011\}\langle 100\rangle$, and a weaker component at $\{4\,4\,11\}\langle 11\,11\,8\rangle$ is revealed (Fig. 6*b*). The maximum of

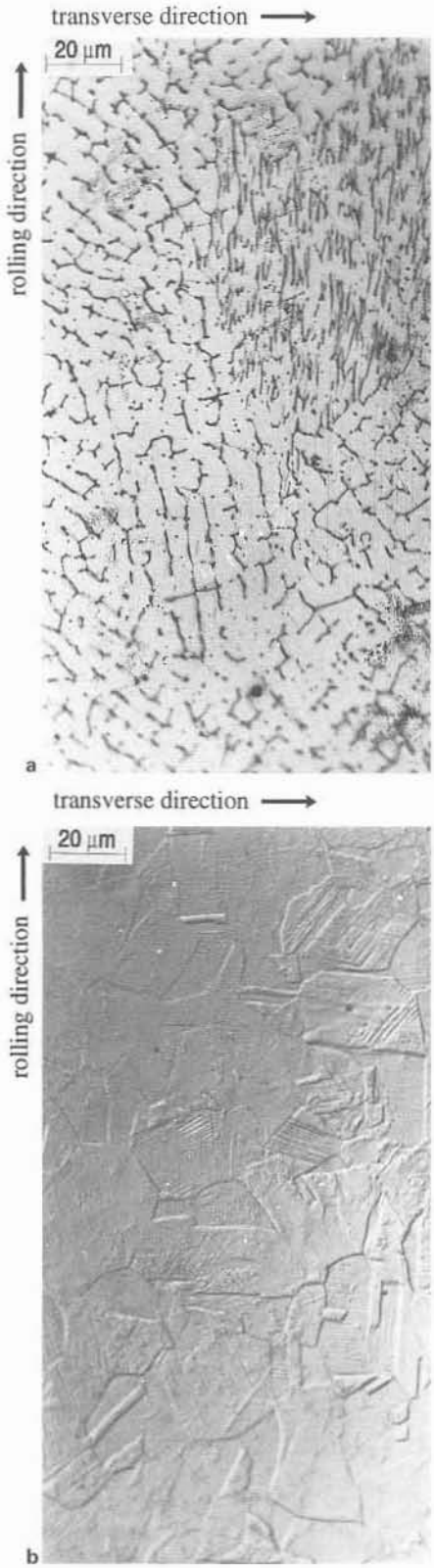

a strip cast austenite; *b* hot rolled austenite

4 Subsurface micrographs of austenitic steel (flat sections)

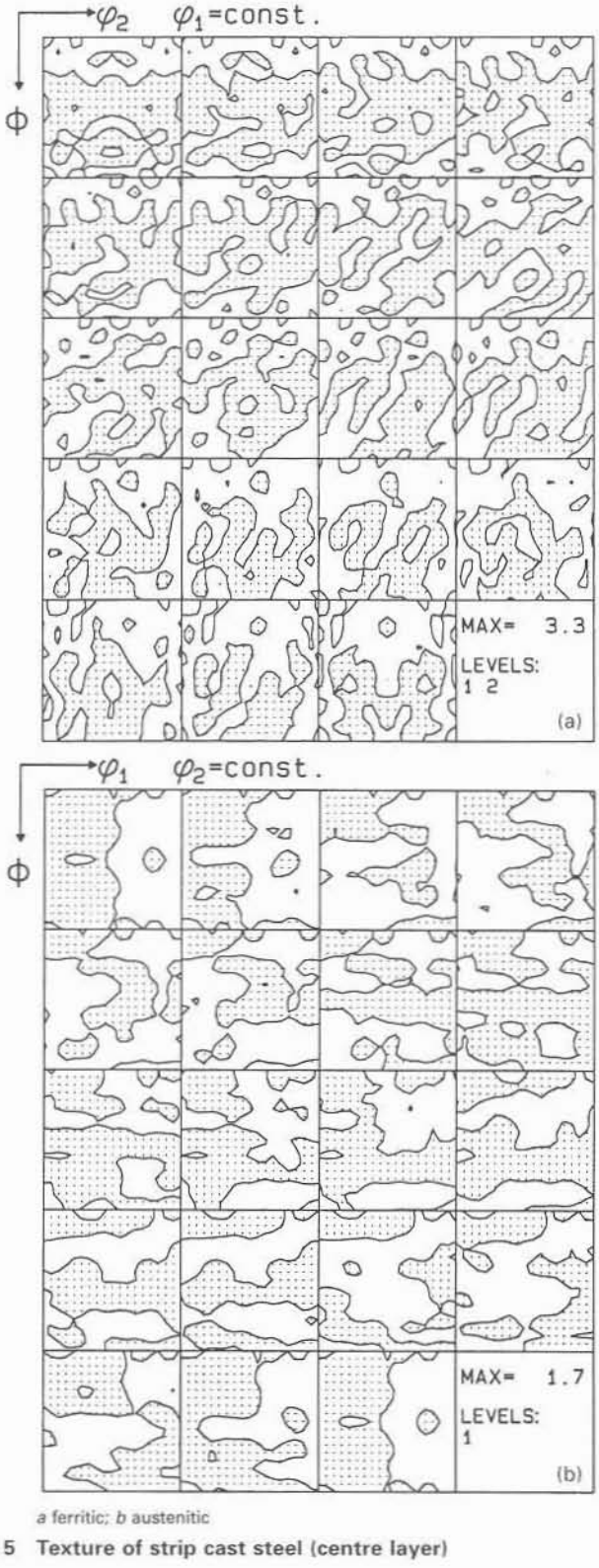

a ferritic; *b* austenitic

5 Texture of strip cast steel (centre layer)

these shear components, in hot rolled ferritic stainless steels, is frequently located at $s = 0{\cdot}7$–$0{\cdot}8$. When the texture profile is inspected with a local through thickness resolution of $\Delta s = 0{\cdot}1$, it can be seen that between the centre and the surface layers there is a continuous decrease in the rolling texture and a steady increase in the typical shear texture components, which represent a characteristic feature of these steels (*see* Fig. 7).[5,6] The resulting profile of the orientation density of the Goss component through various depths is shown in Fig. 8, using data from various steels with 17%Cr content. The occurrence of this type of texture profile within a hot rolled stainless steel band is well known from various ferritic alloys containing 11%Cr, 17%Cr, or 3·4%Si.[5,6,11,15] In Fig. 9 it is shown that with increasing alloy content (especially Cr and Si), i.e. with decreasing volume fraction of phase transformation during cooling after hot rolling, the intensity of the orientation density of the midthickness component $\{001\}\langle 110\rangle$ is enhanced.

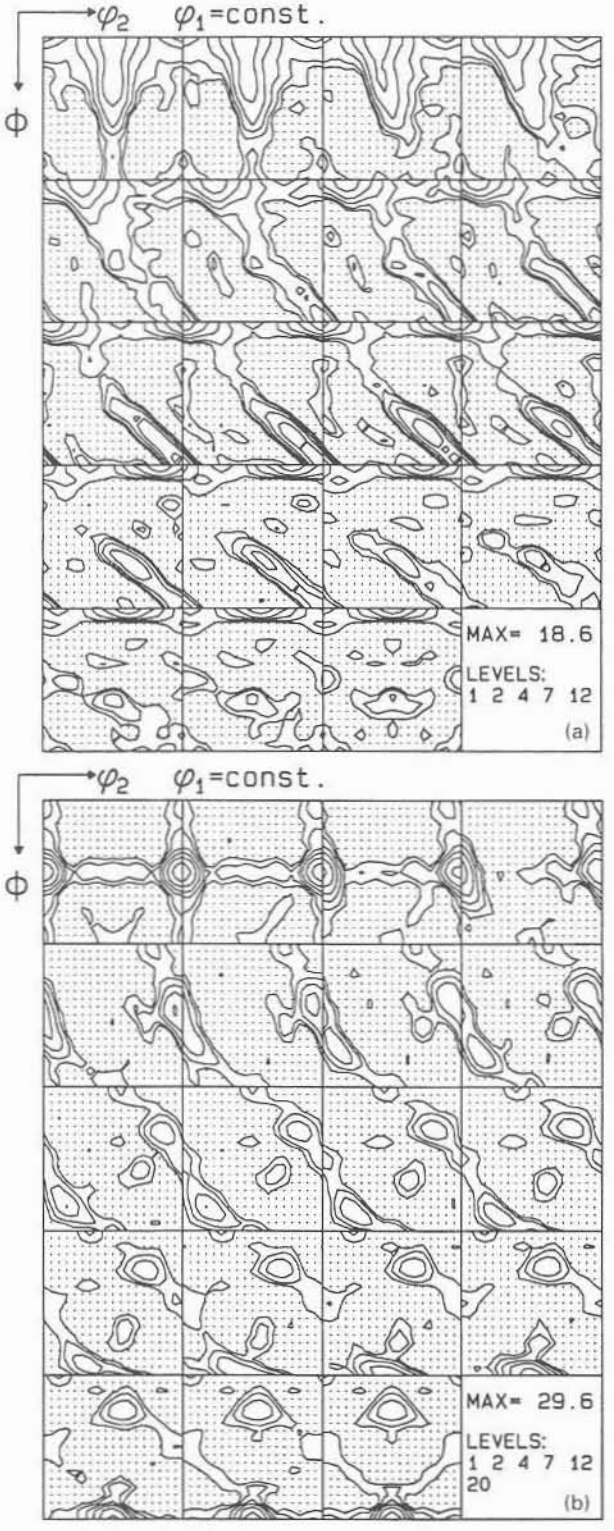

a centre layer; *b* surface layer, *s* parameter = 0·8

6 Texture of hot rolled ferritic steel

The austenitic hot band also reveals an inhomogeneous texture profile through the thickness. Close to the centre layer, i.e. at $s = 0{\cdot}0$ and $s = 0{\cdot}1$, the orientation distribution is characterised by a weak β fibre with a maximum at $\{011\}\langle 211\rangle$, accompanied by the appearance of a weak cube component $\{001\}\langle 100\rangle$ (*see* Fig. 10*a*). In the layer $s = 0{\cdot}2$ the orientations mentioned above are replaced by a nearly random orientation distribution. Close to $s = 0{\cdot}5$–$0{\cdot}6$ a texture transition takes place. Three new orientations, namely a weak $\{001\}\langle 110\rangle$ component, a γ fibre, and a strong $\{112\}\langle 110\rangle$ orientation, which corresponds to the

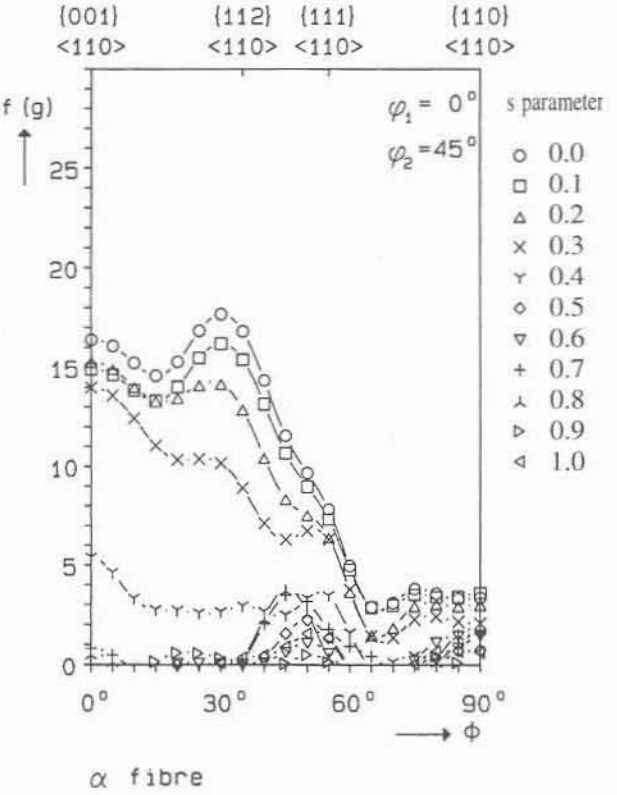

7 Texture of hot rolled ferritic steel (α fibre presentation)

30° about TD rotated rolling component $\{110\}\langle 112\rangle$, are developed (*see* Figs. 10*b* and 11). In the subsurface layers ($s = 0{\cdot}7$–$0{\cdot}8$) the orientation distribution is again random. At the surface ($s = 1{\cdot}0$) a similar texture as in layer $s = 0{\cdot}6$ is developed. In order to describe the through thickness texture profile of the hot rolled austenite, the three shear components which show a maximum orientation density close to $s = 0{\cdot}6$ are chosen as indicators (Fig. 11). It is revealed that the orientation density of all three components shows a similar through thickness variation. Close to the centre layer both orientations are very weak and increase continuously up to layer $s = 0{\cdot}6$. Between $s = 0{\cdot}6$ and $s = 0{\cdot}9$ a decrease, and at the surface again an increase can be seen. This pattern represents the main contrast to the ferritic hot band where the shear components reveal a

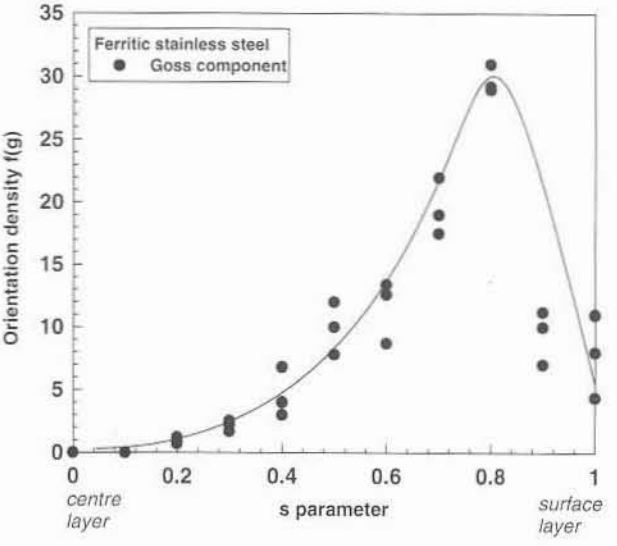

8 Through thickness profile of Goss component {011}⟨100⟩ (ferritic steel)

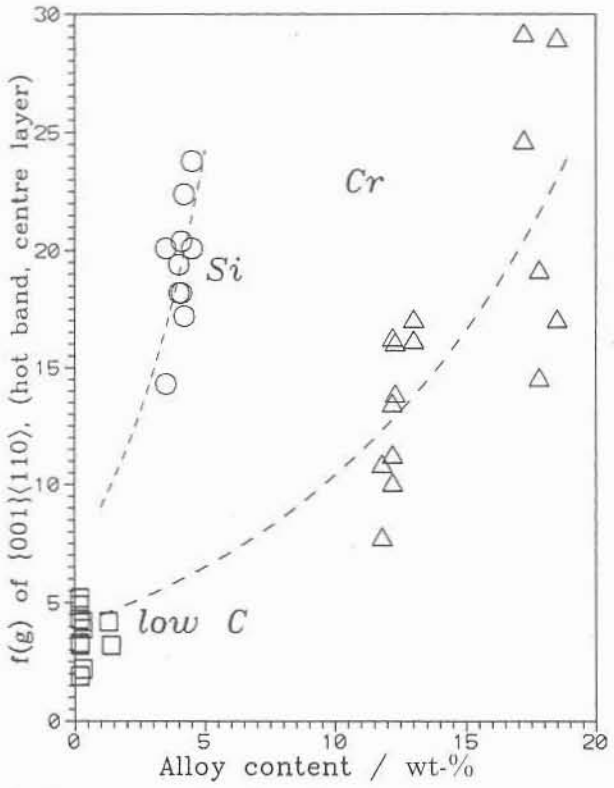

9 Dependence of orientation density of {001}⟨110⟩ component in centre layer of hot rolled ferritic steels on alloy content

maximum at $s = 0{\cdot}8$ and not at $s = 0{\cdot}6$ or $s = 1{\cdot}0$, respectively (*see* Fig. 8).

Discussion

STRIP CASTING

The first important contrast between the textures resulting from the different processing techniques, which is detected for ferritic as well as for austenitic steel, is the nearly random orientation distribution generated during strip casting and the strong and inhomogeneous texture which develops during hot rolling. The almost random textures of both strip cast samples can be explained by the weak growth selection which is attributed to heterogeneous nucleation, i.e. to the high solidification rate on the surfaces of the casting rolls.

As investigated previously,[3,4] for the ferritic steel, where the ridging phenomenon usually deteriorates the surface properties of conventionally hot rolled and subsequently cold rolled and recrystallised steel sheet, the random initial casting texture has a very beneficial effect on the elimination of the ridging phenomenon. The ridging, which occurs after 7% elongation of conventionally processed ferritic hot band, is attributed to the inheritance of the inhomogeneity of the initial texture and microstructure, i.e. to the presence of elongated regions with similar orientations. In strip cast ferritic stainless steels which have a nearly random starting texture, ridging no longer occurs.

HOT ROLLING OF FERRITIC STEEL

The hot rolling textures (Figs. 6 and 10) in both alloys are completely different from the corresponding random strip casting textures (Fig. 5). Owing to the high alloy content, the ferritic steel with 17%Cr content does not undergo a great deal of phase transformation during the last hot rolling passes so that no texture randomisation, as in low C steels, takes place during cooling after hot rolling.

The resulting profile of the ferrite texture through the sheet thickness can be explained by the occurrence of a so called ideal plane strain deformation state ($\varepsilon_{33} = -\varepsilon_{11}$, all other components equal zero) accompanied by recovery instead of recrystallisation in the midthickness layers (Fig. 6*a*) and strong shear deformation close to the surface layers (Fig. 6*b*).[16] The values of the orientation densities

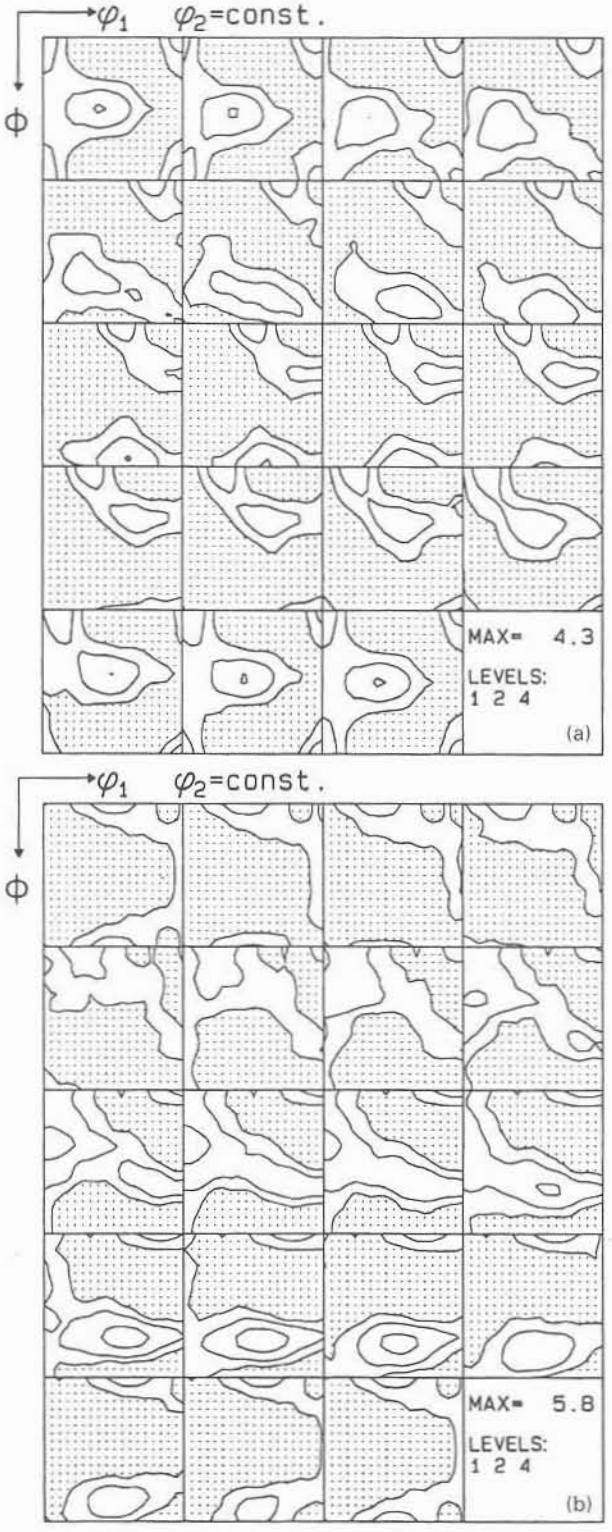

a centre layer; *b* subsurface layer, *s* parameter = 0·6

10 Texture of hot rolled austenitic steel

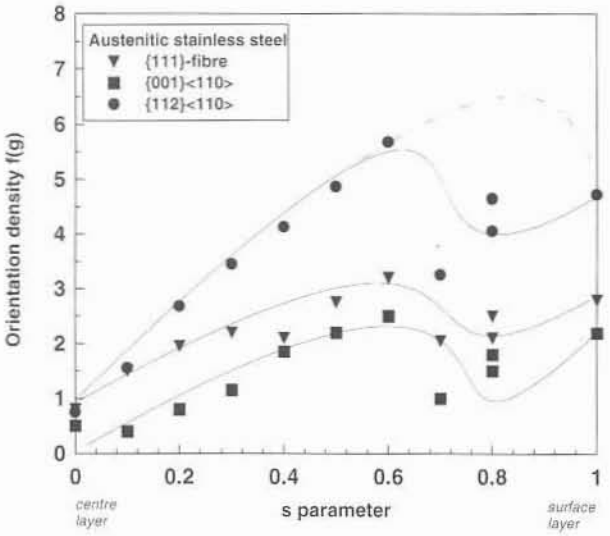

11 Through thickness profile of shear components (austenitic steel)

of the shear components $\{011\}\langle 100\rangle$ (Fig. 8), $\{110\}\langle 112\rangle$, and $\{4\,4\,11\}\langle 11\,11\,8\rangle$ (Fig. 6*b*) at various depths correspond to the profile of the shear strain which results from the influence of the temperature on the flow stress and the through thickness profile of the Zener–Holomon parameter, as calculated by Beynon *et al.*[17] and McLaren and Sellars.[16,18] From these simulations it can also be seen that the centre of the sheet is deformed under ideal plane strain conditions. This leads to the presently observed strong increase of the α fibre, especially the $\{001\}\langle 110\rangle$ orientation in the midthickness layer of the ferritic hot band, which also represents the main texture component in cold rolled ferritic stainless steels.[5,6]

The α fibre texture in the centre layers of the hot band is also considered to be the reason for the ridging phenomenon mentioned above, especially in Fe–17%Cr. As discussed by Hölscher[19] and Bethke *et al.*,[20] the main α fibre components $\{112\}\langle 110\rangle$ and $\{111\}\langle 110\rangle$ both deform by asymmetric activation of glide systems and lead to a resulting ε_{23} shear (2 = TD, 3 = ND). The topological arrangement of these orientations in the elongated hot band morphology leads to the observed macroscopic ridging. Only a reduction of these components in the hot band texture, a change in the deformation mode, or the randomisation of the texture by phase transformation can thus contribute to elimination of the ridging phenomenon.

HOT ROLLING OF AUSTENITIC STEEL

The most relevant feature of the austenitic hot band texture is also, as in the ferritic steel, the course of the through thickness inhomogeneity which is characterised by a weak β fibre, by the occurrence of the cube orientation in the centre layer (Fig. 10*a*), and by a γ fibre, the 45° ND rotated cube orientation, and the $\{112\}\langle 110\rangle$ component close to the surface layers (Figs. 10*b* and 11). As shown in Fig. 11 two maxima of the orientation density of the latter type of texture occur, one at $s \approx 0{\cdot}6$ and a second at $s = 1{\cdot}0$.

According to experimental results by Goodman and Hu,[7] Donadille *et al.*,[8] and Rickert,[9] as well as Taylor simulations by Hirsch and Lücke,[21] the observed β fibre at $s = 0$ (Fig. 10*a*) is a typical rolling texture which results from ideal plane strain deformation of fcc polycrystals at ambient temperatures, although in the present austenitic hot band the maximum orientation density is considerably lower than after cold rolling of comparable alloys. Since complete recrystallisation during or after hot rolling would have removed the detected rolling texture at $s = 0$, this result suggests the possibility that during hot rolling, a high volume fraction of material has only undergone recovery. This, however, would be in contradiction to the observed microstructure, which consists of an equiaxed instead of an elongated recovered grain morphology (Fig. 2), and to the low stacking fault energy (SFE) of the austenitic stainless steel, 21×10^{-3} J m^{-2} (Ref. 22), which suggests a strong tendency for recrystallisation instead of recovery. It is thus more likely that recrystallisation has occurred during the first hot rolling passes and that the weak detected β fibre texture was developed during the last rolling passes, i.e. after considerable cooling of the sheet where the temperature of the band and the stored energy imposed by the last rolling pass were too low for recrystallisation. This conclusion is in good agreement with the observed low orientation density, because the recovery of rolled material would have led to a much stronger texture maximum. Owing to the low SFE of the austenite, the occurrence of the cube orientation (Fig. 10*a*) in the centre layer of the austenitic hot band is attributed to recrystallisation.

The textures in the other layers of the austenitic alloy are different when compared with that which is observed at $s = 0$. Whereas in some layers a random texture occurs, at $s = 0{\cdot}6$ and $s = 1$ (Fig. 11) a γ fibre, a $\{001\}\langle 110\rangle$, and a $\{112\}\langle 110\rangle$ orientation are detected. All three orientations are well known from inhomogeneously rolled Al and represent typical orientations which are attributed to shear deformation.[23–25] According to Mao,[25] the $\{112\}\langle 110\rangle$ component results from the $\{011\}\langle 211\rangle$ orientation, which represents the strongest ideal plane strain rolling component in fcc metals with low SFE values and which has been rotated 30° about the TD owing to the rotation of the strain state. The through thickness profile of the austenitic shear components thus corresponds to the texure profile of the comparative shear orientations of the hot rolled ferritic stainless steel (Fig. 8). However, whereas in the ferrite the strongest shear and thus also the highest orientation densities of the corresponding texture components occur at $s = 0{\cdot}7$–$0{\cdot}8$, in the austenitic hot band the maximum of the shear texture is locally split into one peak at $s = 0{\cdot}6$ and a second peak at $s = 1$. At $s = 0{\cdot}7$–$0{\cdot}8$ even a local minimum is detected (Fig. 11). In order to explain this deviation of the austenitic texture profile, it is assumed that the maximum of the shear was truly positioned in the range $s = 0{\cdot}7$–$0{\cdot}8$ as suggested by the ferrite and as predicted by simulations[16–18] (schematically indicated by the dotted line in Fig. 11). However, since this implies a higher local deformation, i.e. a higher stored dislocation energy, it is assumed that in these layers recrystallisation could take place more easily, leading to randomisation of the texture.

Conclusions

The crystallographic texture of two industrially strip cast and two hot rolled stainless steels, one with 17%Cr content (ferritic) and one with 18%Cr and 8·5%Ni content (austenitic) was investigated through the thickness of the specimens. The texture of both strip cast alloys was nearly random in all the layers examined which was attributed to the weak growth selection, due to the high solidification rate on the surfaces of the casting rolls. In the hot bands of both alloys a strong texture profile was found, showing orientations stemming from ideal plane strain rolling deformation in the centre layers and strong shear texture components close to the surface. These textures were interpreted in terms of the through thickness strain profile which occurs during industrial hot rolling.

Acknowledgements

The author gratefully acknowledges the kind support by the strip casting research group of Krupp-Hoesch Stahl AG, especially by Dr M. Dubke and Dr M. Hölscher.

References

1. K. OHNO, H. TANAKA, T. SASAKI, M. DUBKE, H. J. FUNK, K. H. HANKE, H. PFEIFER, and R. HENTRICH: in Proc. Int. Conf. on 'New smelting reduction and near net shape casting technologies for steel', Pohang, Korea, 1990, The Korean Institute of Metals and The Institute of Metals, p. 682.
2. R. HENTRICH, M. DUBKE, H. J. FUNK, K. H. HANKE, J. LOH, and S. KUHLMANN: *Stahl Eisen*, 1991, **51**, 111.
3. D. RAABE, M. HÖLSCHER, M. DUBKE, H. PFEIFER, H. HANKE, and K. LÜCKE: *Steel Res.*, 1993, **64**, 359.
4. D. RAABE, M. HÖLSCHER, M. DUBKE, and K. LÜCKE: in Proc. Int. Conf. on 'Hot and cold working of stainless steels', (ed. N. D. Ryan *et al.*), Quebec, Canada, August 1993, The Metallurgical Society of the Canadian Institute of Mining and Metallurgy and Petroleum, p. 3.
5. D. RAABE and K. LÜCKE: *Mater. Sci. Technol.*, 1993, **9**, 302.
6. M. HÖLSCHER, D. RAABE, and K. LÜCKE: *Steel Res.*, 1991, **62**, 567.
7. S. R. GOODMAN and H. HU: *Trans. AIME*, 1964, **230**, 1413.
8. C. DONADILLE, R. VALLE, P. DERVIN, and R. PENELLE: *Acta Metall.*, 1989, **37**, 1547.
9. T. RICKERT: *Mater. Sci. Forum*, 1993, **157–162**, 2017–2024.
10. C. D. SINGH, V. RAMASWAMY, and C. SURYANARAYANA: *Textures Microstruct.*, 1991, **13**, 227.
11. D. RAABE and K. LÜCKE: *Scr. Metall.*, 1992, **26**, 1221.
12. L. G. SCHULZ: *J. Appl. Phys.*, 1949, **20**, 1030.
13. H. J. BUNGE: in 'Texture analysis in materials science', 1982, London, Butterworths.
14. D. RAABE, M. HÖLSCHER, F. REHER, and K. LÜCKE: *Scr. Metall.*, 1993, **29**, 1.
15. D. RAABE and K. LÜCKE: *Mater. Sci. Forum*, 1993, **157–162**, 597–610.
16. A. J. McLAREN and C. M. SELLARS: *Mater. Sci. Technol.*, 1992, **8**, 1090.
17. J. H. BEYNON, A. R. S. PONTER, and C. M. SELLARS: in Proc. Conf. 'Modelling in metal forming', 321; 1988, London, Kluwer Academic.
18. A. J. McLAREN and C. M. SELLARS: in Proc. Int. Conf. on 'Hot and cold working of stainless steels', (ed. N. D. Ryan *et al.*), Quebec, Canada, August 1993, The Metallurgical Society of the Canadian Institute of Mining and Metallurgy and Petroleum, p. 107.
19. M. HÖLSCHER: PhD thesis, RWTH Aachen, 1987.
20. K. BETHKE, M. HÖLSCHER, and K. LÜCKE: *Mater. Sci. Forum*, 1993, **157–162**, 1137–1144.
21. J. HIRSCH and K. LÜCKE: *Acta Metall.*, 1988, **36**, 2863.
22. R. E. SCHRAMM and R. P. REED: *Metall. Trans.*, 1975, **6A**, 1345.
23. J. HIRSCH: in 'Hot deformation of aluminium alloys', (ed. T. G. Langdon *et al.*), 379; 1991, Warrendale, PA, TMS.
24. M. HÖLSCHER, D. RAABE, and K. LÜCKE: *Acta Metall.*, 1994, **42**, 879–886.
25. W. MAO: PhD thesis, RWTH Aachen, 1988.